2004 International Symposium on Nonlinear
Theory and its Applications (NOLTA2004)
Fukuoka, Japan, Nov. 29 - Dec. 3, 2004

Comparative Study of Entrainment in Circadian Clock Systems

Hisa-Aki Tanaka and Tomoki Maegawa

Department of Electronic Engineering, The University of Electro-Communications (UEC)
1-5-1 Choufugaoka, Choufu-shi, Tokyo 182-8585 Japan
Email: htan@synchro3.ee.uec.ac.jp

Abstract—The phase dynamics (; phase equation) is analyzed in the interlocked feedback model of *Drosophila* circadian systems with weak light input. From the phase equation, range of entrainment can be obtained systematically for light-dark cycle inputs, and for various light input patterns. These theoretical predictions are verified in the simulation results of entrainment, and explain how the range of entrainment is affected by the input patterns. Based on this framework, inverse problems on the entrainment characteristics are formulated and some insight is obtained.

1. Introduction

Computer simulations are now essential in analyzing large-scale and complex systems in science and engineering. Tools like SPICE and NEURON have been elaborated and widely used. However, data produced by them does not necessarily lead to total understanding of the system, because the simulation model itself has become too complex to follow. Such bottleneck emerges in recent circadian rhythm study where increasing number of clock proteins and mRNAs are involved in molecular-based simulation models.

In this presentation, we introduce a method of phase reduction to analyze the *Drosophila* circadian clock systems and attempt to gain a systematic understanding of entrainment characteristics, suggesting a protocol controlling the entrainment characteristics.

2. Interlocked Feedback Model

At molecular level, the *Drosophila* clock system involves several genes; period (*per*), timeless (*tim*), *Drosophila* clock (*dClk*), Cycle (*Cyc*) and double time (*dbt*), and three genes are rhythmically expressed; *per*, *tim* and *dClk*. Leloup and Goldbeter [1] proposed a delayed negative feedback loop model involving *per*, *tim* and repressed transcription of *per* and *tim* by PER-TIM complex. This model has stimulated more elaborated models involving other genes. At present, the interlocked feedback model [2, 3] is one of the most sophisticated and convincing models. Adding to the *per* and *tim* rhythmic expression in the model by Leloup and Goldbeter, the interlocked feedback model accounts for the rhythmic expression of *dClk*, and also

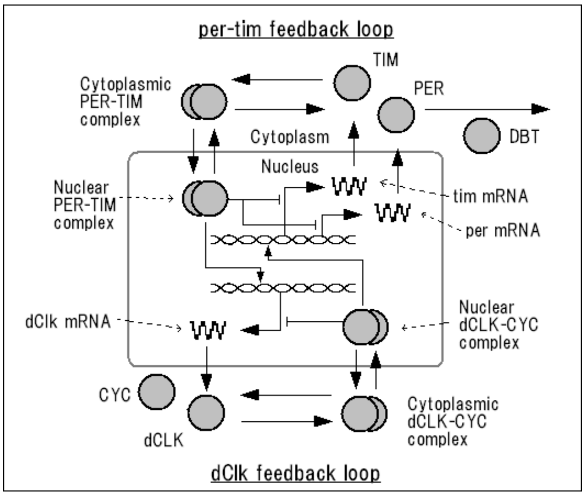

Fig.1 Interlocked feedback model of *Drosophila* circadian rhythm[3].

explains how decrease of *per* and *tim* mRNA levels takes place in mutants lacking PER or TIM function.

2.1. Mathematical Model Based on the Interlocked Feedback Model

Ueda et al [3] formulated a mathematical model based on the interlocked feedback model, which is schematized as in Fig. 1. As shown in Fig.1, a *per-tim* feedback loop and a *dClk* feedback loop are interacting by derepressing its own mRNA transcription with PER-TIM, and repressing with dCLK-CYC respectively. This model defines ten-variable ordinally differential equations, in which each variable represents the temporal concentration of the protein or mRNA. The kinetics of the mRNA transcription and the protein translation, degradation and nuclear transportation are described with Hill-type equations and Michaelis-Menten-type equations, respectively. Kinetic constants are chosen to yield a 24 hr circadian period in constant darkness conditions.

2.2. Entrainment by Light Input

To characterize the response of the circadian clock system to the light input, a PRC (phase resetting curve) is often measured experimentally. In the interlocked feedback model as well as the Leloup and Goldbeter model [1], the effect of light inputs is modeled by the temporal increase of the degradation coefficient of TIM (; D_4 in [3]). This simple modeling produces numerically obtained PRCs, showing a nice fit to the experimental PRCs. In this study we focus on this model to analyze the effects of various light inputs systematically, although our analytical method is amenable to more elaborated models for light input effects.

3. Phase Dynamics in the Interlocked Feedback Model

Mathematically speaking, self-sustained oscillations in the interlocked feedback loop can be characterized as a limit cycle in the ten-variable phase space. This implies that the system dynamics can be reduced to a natural phase of the oscillations under weak light input conditions. The reduced dynamics of the phase can be defined as phase equations, which can be obtained by solving the adjoint variational equation about the limit cycle and by using the averaging method [4], in principle.

3.1. Derivation of Phase Equations

As mentioned above, the derivation of the phase equation is straightforward, once the limit cycle and the solution of the adjoint variational equation is obtained. However, in practice, this method (; the adjoint eigenfunction method) requires much computational cost especially for highly nonlinear, large-scale systems such as the interlocked feedback model. Here, instead of this straightforward method, we employ an indirect method deriving the phase equations; the impulse response method [5].

In using, the impulse response method, we first compute the linear response region (LRR), in which the amount of phase shifts is proportional to the input strength (; impulse height). In this region, the PRC is uniquely determined under a certain scaling. Here, we call this scaled PRC as the impulse sensitivity function (ISF) per Hajimiri [6]. Examples of the LRR and PRC in this study are shown in Fig.3 and Fig.4, respectively. Using this ISF, we can obtain the phase equation of the interlocked feedback model as

$$\frac{d\theta(t)}{dt} = \omega_0 + H(\theta(t) - \tilde{\theta}(t)), \quad (1)$$

with

$$\frac{2\pi}{T_0}\int_0^{T_0} \frac{\Gamma(\omega_0 t + \phi)}{S} R(\omega_0 t + \tilde{\phi})\, dt \equiv H(\phi - \tilde{\phi}), \quad (2)$$

where $\theta(= \omega_0 t + \phi)$ and $\tilde{\theta}(= \omega_0 t + \tilde{\phi})$ represent the oscillation phase of Per_m and the light input, respectively. $\Gamma(\cdot)$, $R(\cdot)$, and S represent the PRC, the light input waveform, and the normalization constant (; pulse height × width), respectively. ω_0 is the natural frequency of the circadian rhythm and $\omega_0 = \frac{2\pi}{T_0}$ holds.

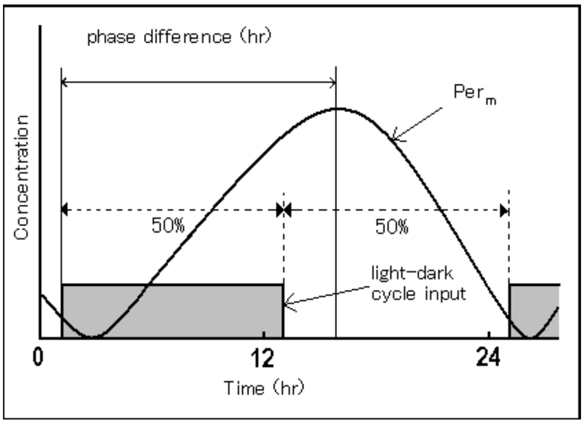

Fig.2 Phase difference between the circadian rhythm of Per_m concentration and the light-dark cycle input intensity.

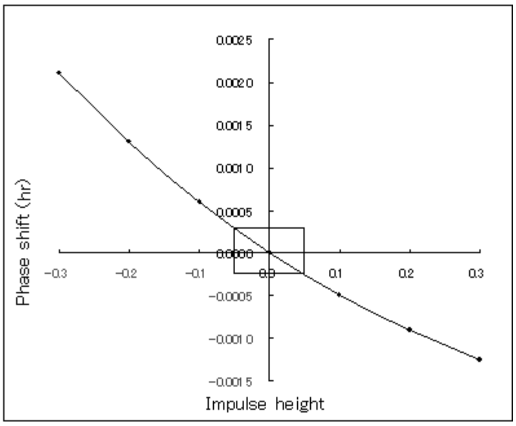

Fig.3 Relationship between phase shift and impulse height. The solid square defines the LRR.

The phase difference $\theta - \tilde{\theta}$ is defined as in Fig.2 such that $\theta - \tilde{\theta}$ becomes 0 when the frequency of the input coincides to the natural frequency of the circadian rhythm.

3.2. Effect of Input Pattern on the Entrainment Range

Now the entrainment characteristics is reduced to the function $H(\cdot)$ in Eq. (1). The obtained functions $H(\cdot)$ are shown in Fig. 5, where the waveform clearly depends on the input waveform. Theoretically obtained ranges of phase shift are [-7.736, 6.515], [-6.058, 5.965], and [-6.905, 5.118], for the chopped si-

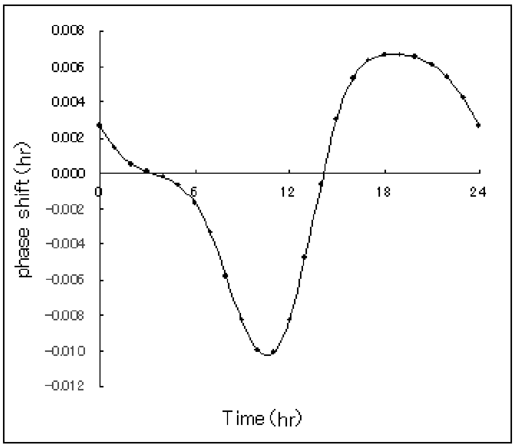

Fig.4 Phase shifts with respect to light impulse timing.

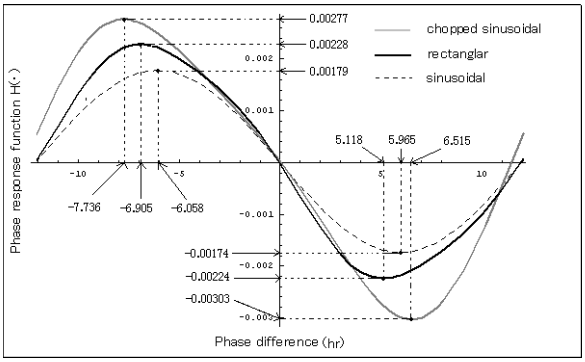

Fig.5 Entrainment characteristics for three different photonic inputs (theoretical predictions).

nusoidal input, sinusoidal input, and rectangular input, respectively. (In the chopped sinusoidal input, the maximum is $\frac{2}{\pi} \times 0.03$ and the minimum is 0. In the sinusoidal input, the amplitude is 0.015, the maximum is 0.03, and the minimum is 0. In the rectangular input, the maximum is 0.03 and the minimum is 0.)

The entrainment characteristic directly obtained by the simulations is shown in Fig. 6, where the data shows a complete agreement to the above theoretical prediction of the phase shift and range of entrainment.

From the above results, we observe that
(i) the phase equation provides systematic predictions on the entrainment characteristics of the interlocked feedback model, and
(ii) the entrainment characteristics shows a clear dependence on the input pattern.

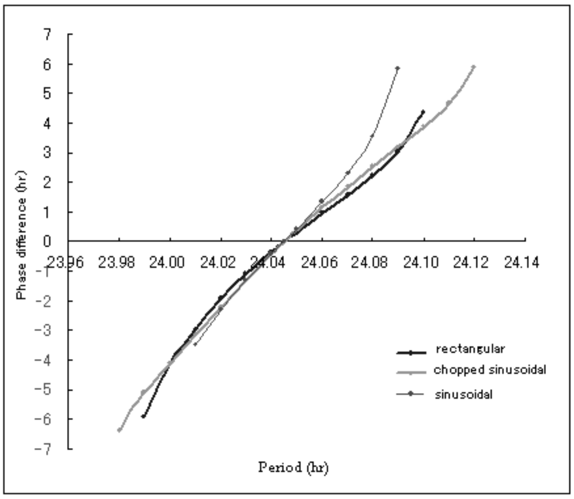

Fig.6 Entrainment characteristics for three different photonic inputs (simulation results).

3.3. Inverse Problem of the Entrainment Characteristics

Motivated by the result (ii), a certain inverse problem is formulated as :
(a) for a given entrainment characteristics $H(\phi - \tilde{\phi})$, does the input $R(\tilde{\phi})$ exist or not ? And,
(b) what kind of the input pattern $R(\tilde{\phi})$ realizes a maximum range of entrainment ?

To analyze such issues, it is convenient to express $\Gamma(\phi)$ and $R(\tilde{\phi})$ by the Fourier series as :

$$\Gamma(\phi) = \sum_{k=0}^{N}(a_k \cos k\phi + b_k \sin k\phi). \tag{3}$$

Input:

$$R(\tilde{\phi}) = \sum_{k=0}^{N}(x_k \cos k\tilde{\phi} + y_k \sin k\tilde{\phi}). \tag{4}$$

From eqs. (2), (3), and (4), we obtain

$$H(\phi - \tilde{\phi}) = \frac{1}{2}\sum_{k=0}^{N}[(a_k x_k + b_k y_k)\cos\{k(\phi - \tilde{\phi})\} + (-a_k y_k + b_k x_k)\sin\{k(\phi - \tilde{\phi})\}]. \tag{5}$$

If a given entrainment characteristics is expressed as

$$H(\phi - \tilde{\phi}) = \sum_{k=0}^{N}[\alpha_k \cos\{k(\phi - \tilde{\phi})\} + \beta_k \sin\{k(\phi - \tilde{\phi})\}], \tag{6}$$

then the following equations must be satisfied.

$$\begin{aligned} a_k x_k + b_k y_k &= 2\alpha_k, \\ -a_k y_k + b_k x_k &= 2\beta_k, \ (k = 0, \cdots, N). \end{aligned} \tag{7}$$

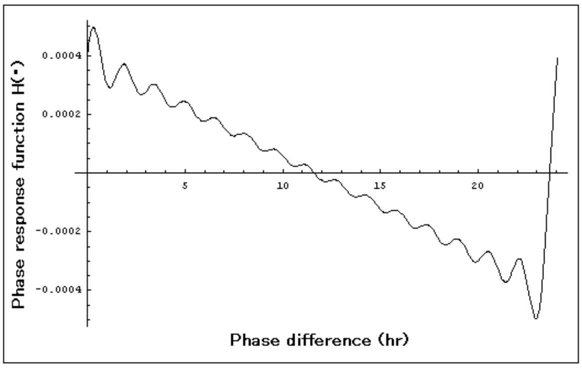

Fig.7 Sawtooth-like phase response function $H(\phi-\tilde{\phi})$.

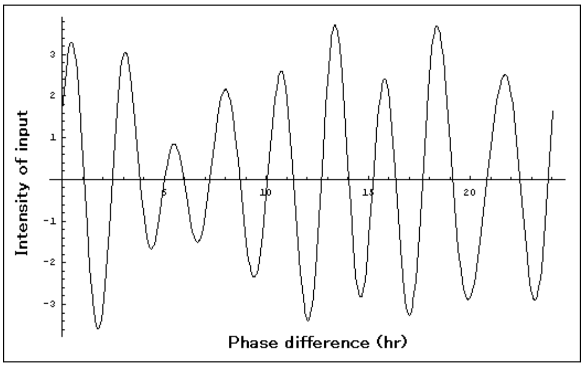

Fig.8 Resulting input waveform $R(\tilde{\phi})$.

In the above situation (a), the unknown (x_k, y_k) can be uniquely determined from eqs. (7) for given coefficients (a_k, b_k) and (α_k, β_k).

In Fig.5 we observe that the entrainment range becomes the widest for the case of a chopped sinusoidal input. In this case, the range of stable phase difference is also the largest among the three input patterns. Then, we have one natural question as: what kind of input pattern realizes the (ideally) largest phase difference ? The limiting case can be a sawtooth-like phase response function $H(\phi - \tilde{\phi})$ as shown in Fig. 8, where the phase difference becomes $[-\pi, \pi]$. (In this particular example, the order N is set to 10 as the number of date points in the ISF $\Gamma(\cdot)$ is limited.)

The resulting input $R(\tilde{\phi})$ realizing the sawtooth-like $H(\phi - \tilde{\phi})$ is shown in Fig. 8. We observe that this $R(\tilde{\phi})$ takes negative value, which contradicts to the 'positive' intensity. Adding to this, the amplitude of $R(\tilde{\phi})$ in Fig. 8 becomes larger than 3, which is far beyond the LRR (which is less than 0.05). Thus, in this particular example, the input $R(\tilde{\phi})$ does not exist and the sawtooth-like phase response function cannot be realized.

For the above issue (b), a hint for practical approach is obtained [7], which will be explained in our presentation.

Acknowledgments

The authors would like to thank Dr. Takashi Shimada, Dr. Gen Kurosawa, and Dr. Hiroki R. Ueda for their fruitful suggestions and comments.

References

[1] J.C. Leloup and A. Goldbeter, "A Model for Circadian Rhythms in Drosophila Incorporating the Formation of a Complex between the PER and TIM proteins," Journal of Biological Rhythms, 13, 70-78, 1998.

[2] N.R. Glossop, L.C. Lyons, and P.E. Hardin, "Interlocked feedback loops within the Drosophila circadian oscillator, Science 286," 766-768, 1999.

[3] H.R. Ueda, M. Hagiwara, and H. Kitano, "Robust Oscillations within the Interlocked Feedback Model of Drosophila Circadian Rhythm," J. Theor. Biol. 210, 401-406, 2001.

[4] Y. Kuramoto, Chemical Oscillations, Waves, and Turbulence, Dover Pubns, 1984.

[5] H. Tanaka, A. Hasegawa, H. Mizuno, and T. Endo, "Synchronizability of Distributed Clock Oscillators," IEEE Trans on Circuits and Systems-I:Fundamental Theory and Applications," 49, 1271-1278, 2002.

[6] A. Hajimiri and T.H. Lee, "A General Theory of Phase Noise in Electrical Oscillators," IEEE Trans on Solid-State Circuits, 33, 179-194, 1998.

[7] T. Shimada, private communication, 2004.